Materials Advances

ROYAL SOCIETY OF CHEMISTRY

PAPER

View Article Online
View Journal | View Issue

Cite this: *Mater. Adv.*, 2022, 3, 7132

Design of an experimental study of high through-plane thermal conductivity hybrid epoxy composite insulation with superior dielectric strength†

Hiep Hoang Nguyen, [ab] Antigoni Konstantinou,[b] Yifei Wang, [b] JoAnne Ronzello,[b] Kerry Davis [b] and Yang Cao *[ab]

Received 26th May 2022,
Accepted 26th July 2022

DOI: 10.1039/d2ma00592a

rsc.li/materials-advances

Thermally conductive polymers are highly desired as electrical insulation materials in power-electronic and electrical machines toward high power density and payload efficiencies. This paper investigates the thermal conductivity of hybrid epoxy composites containing talc nanoclay, boron nitride (BN) clusters, and zinc oxide (ZnO) particles using the Design of Experiment (DoE) approach. A statistical model of the composite thermal conductivity based on the compositions of the components has been established with an *R*-squared of 98.17%. The effects of shapes, sizes, filler thermal conductivity, and the structured network of the fillers are discussed. The structured edge-connecting BN nanosheets endowed in nanostructured BN-clusters play a critical role in composite thermal conductivity enhancement. The thermal conductivity with the optimized formulation could reach 1.3 W m^{-1} K^{-1}, which is 6× higher than that of neat epoxy resin, while maintaining superior dielectric properties. The results of DoE analysis can be widely applied to the design of polymer composites with optimal formulations.

1. Introduction

Epoxy resin is widely used in electrical and electronic industries, in electrical apparatus and devices, electronic packaging, batteries, *etc.*, due to its excellent electrical insulation characteristics, light weight, excellent thermal-, mechanical-, and chemical-resistance, good adhesion, and easy processing.[1–4] In addition to serving as electrical insulation which electrically isolates the current-carrying conductors to grounded parts, epoxy resin is also a medium for heat dissipation from the conductors which are the main heat source in the devices. However, epoxy resin is limited by its low thermal conductivity of only ~0.2 W m^{-1} K^{-1}.

Effective heat dissipation is critical to the power handling capacity, reliability, and life expectancy of the devices. It has been demonstrated that by enhancing the thermal conductivity of the groundwall insulation material of rotating machines from 0.2 W m^{-1} K^{-1} to 0.7 W m^{-1} K^{-1}, the maximum temperature of the copper conductors drops by 40 °C and a significant 26% increase in power density can be achieved.[5,6] Additionally, the operating temperature seriously impacts the device lifetime. When the operating temperature decreases by 10 °C, the life expectancy of the insulation systems can be 2× longer.[7]

To achieve high thermal conductivity, developing advanced composites by introducing thermally conductive fillers into an epoxy matrix is an effective way. High thermally conductive fillers include metals (aluminum, silver, iron, copper, and gold/palladium),[8,9] ceramics (silicon carbide, magnesium oxide, alumina, zinc oxide, boron nitride, nanoclays, and aluminum nitride),[10–14] and carbon-based materials (graphite, carbon nanotubes, and carbon black).[15–17] Unlike metallic particles and carbon based materials which could lead to a high electrical conductivity of the nanocomposites, ceramic materials possessing excellent electrical insulation properties become good candidates for electrical insulation applications.[18–20] In recent years, two-dimensional (2D) nanoclay is widely used in dielectric applications, offering enhanced discharge resistance, dielectric properties, mechanical properties, low cost, and commercial availability.[20,21] BN is also a platelet-like material, commonly used in various critical industrial applications owing to its high thermal conductivity, low dielectric loss, and high lubriciousness. However, nanoclays and BN platelets suffered from anisotropic thermal conductivity. For example, while the in-plane thermal conductivity of hexagonal BN (hBN) was

[a] *Electrical and Computer Engineering, University of Connecticut, 371 Fairfield Way, Storrs, CT 06269, USA. E-mail: yang.cao@uconn.edu*
[b] *Electrical Insulation Research Center, Institute of Materials Science, University of Connecticut, 97 North Eagleville Road, Storrs, CT 06269, USA*

† Electronic supplementary information (ESI) available. See DOI: https://doi.org/10.1039/d2ma00592a

estimated to be 300–550 W m^{-1} K^{-1},[22] or 751 W m^{-1} K^{-1} for one-atom-thin hexagonal BN,[23] the through-plane thermal conductivity is only 2–3 W m^{-1} K^{-1}.[17] Therefore, the composite thermal conductivity will largely depend on the orientation of the platelets. To take the advantage of high in-plane thermal conductivity and improve the isotropic thermal conductivity of hBN, structured spherical BN clusters were developed by bonding multiple hBN platelets at their edges in random directions to increase the effective conduction path in all directions.[24–26]

It shall be noted that structure/composition engineering plays a crucial role, as the combination of various fillers may lead to synergistic, antagonistic, or insignificant effects on the effective thermal conductivity of the composite. Also, in various applications, it is of great importance to acquire a range of filler contents that offer a targeted composite thermal conductivity value so that other properties can be tuned and achieved accordingly. Using a mixture Design of Experiment (DoE) for systematically seeking the relationships between multiple variables and output responses has been demonstrated to be an effective and adequate method with minimum time, labor, and resources.[27–32]

In this paper, the thermal conductivity of hybrid epoxy composites designed for high torque density propulsion motors that compose 2D nanoclays, spherical BN cluster particles, and hexagonal prism ZnO particles is studied. Through the mixture DoE, the effects of content, the shape, size, the thermal conductivity of each filler, and the possible interactions between two components on the composite thermal conductivity are statistically investigated. Moreover, to elucidate the effectiveness of the structured thermally conductive paths endowed in edge-connecting BN clusters, an epoxy composite with homogeneously dispersed BN platelets is studied as a reference. The heat transport mechanism in the two cases is studied using the theoretical Agari–Uno model. Finally, the dielectric breakdown strength, dielectric constant, and dissipation factor of the designed composites are evaluated to examine their dielectric performances.

2. Materials and methodology

2.1 Materials

For the preparation of composites, epoxy resin (Bisphenol A-Epichlorohydrin/Phenol – Formaldehyde, provided by VonRoll USA) was used as the base polymer. This is a high-performance one-part epoxy resin, specifically designed for groundwall insulation of large motors and generators. Ultrafine nanoclay with a 2D layered crystalline structure was provided by IMERY. ZnO particles were purchased from G.H. Chemicals. Specially treated BN cluster particles, designed to significantly increase the thermal conductivity of the composite, were provided by Momentive. The BN platelet powders with a dimension of 800 nm were purchased from US Research Nanomaterials, Inc. The properties of epoxy resin and fillers are listed in Table 1.

Table 1 Properties of the components used in the epoxy composites

Components	Average particle size (μm)	Theoretical density (g cm^{-3})	Thermal conductivity (W m^{-1} K^{-1})
Epoxy resin	N/A	1.2	~0.2
Talc nanoclay	2	2.76	10.69 ($\lambda_{//}$) 1.76 ($\lambda_{\perp}$)
BN cluster	60	2.1	300–550 ($\lambda_{//}$)
BN platelet	0.8		2–3 ($\lambda\perp$)
ZnO	0.3–1	5.61	50

2.2 Sample preparation and experimental procedure

Prior to processing, all fillers were pre-dried at 140 °C for 12 hours to remove residual moisture. The fillers were mixed in the epoxy matrix by a high shear planetary centrifugal Thinky® mixer. The degassing of the mixture was carried out at the same time under a vacuum of 30 kPa. After mixing, the homogeneous, bubble-free mixture was cast in circular molds with a diameter of 5 cm by the natural flowing method, which was then cured in a convection oven. In the curing process, the temperature was incrementally increased up to 160 °C with an average ramping rate of 1 °C min^{-1}, then kept isothermally at 160 °C for 12 hours, followed by natural cooling down to room temperature. The solid-state samples obtained after curing were then machined down to a thickness of 5 mm for thermal conductivity measurements and a thinner thickness for electrical testing.

2.3 Scanning electron microscopy

The morphologies of the fillers and the distribution of the fillers in the epoxy composite were characterized with Teneo LV Scanning Electron Microscopy (SEM). To reveal the elemental composition, Energy Dispersive X-Ray spectroscopy (EDX) coupled with SEM was implemented. To avoid the charge accumulation which affects the SEM image quality, a thin layer of Au/Pd (thickness of ~3 nm) was sputter-coated on the sample, which was grounded by a copper tape.

2.4 Thermal conductivity measurement

The thermal conductivity measurement was conducted using the TA DTC-300 according to the ASTM E1530 standard. The measurement principle is based on the guarded hot plate method. The sample is placed between two polished metal surfaces, each controlled at a different temperature. While the temperature of one metal surface is set lower than the sample temperature by 15 °C, that of the other is higher by 15 °C. The thermal conductivity is determined by dividing the temperature difference across the sample along with the output from the heat flux transducer by the sample thickness.[33]

To minimize the thermal contact resistance between the measured sample and measuring surfaces, a thin layer of thermally conductive compound is applied on both sides of the sample, which is under a pneumatic compressive load of 20 psi.

2.5 Mixture design of the experiment

To systematically investigate the relationship and establish a statistical model between the concentration of the components in wt% as input variables and the composite thermal conductivity as an output response, mixture DoE was implemented using a Minitab software tool package.

The mixture contains epoxy resin as the polymer matrix and three functional fillers, including 2D nanoclay, BN cluster particles, and ZnO particles. From the screening experimentations, the constraints are set on each component to ensure all desired properties be met. Therefore, an extreme vertices mixture,[34] in which the designed points cover only an appropriate sub-portion of interest, was implemented with a degree of 2. In the mixture, the amount of epoxy resin – X_1 (wt%), talc – X_2 (wt%), BN cluster particles – X_3 (wt%), and ZnO – X_4 (wt%) was determined as follows:

$$60 \leq X_1 \leq 75 \quad (1)$$

$$20 \leq X_2 \leq 30 \quad (2)$$

$$5 \leq X_3 \leq 20 \quad (3)$$

$$0 \leq X_4 \leq 15 \quad (4)$$

$$25 \leq X_2 + X_3 + X_4 \leq 40 \quad (5)$$

In the mixture design, the sum of $X_1 + X_2 + X_3 + X_4$ is always 1 (or 100 wt%). The lower constraint of the total percentage of the fillers in eqn (5) was set at 25 wt% to maximize the advantage of functional fillers on the epoxy composite properties. The upper limit is 40 wt% to ensure satisfactory sample processing quality and reproductivity. A higher concentration of the fillers could increase the viscosity of the mixture, which aggravates the mixing process and leads possibly to the formation of cracks after curing.

The design space, generated by Minitab, contains 22 formulations. Specimens of each formulation were fabricated according to the procedure presented in the previous section. After mixing and curing, the thermal conductivity of each formulation was measured in accordance with the ASTM E1530 standard. The experimental results of the thermal conductivity measurements were then fed into the DoE analysis, in which a mathematical relationship between the thermal conductivity and the weight percentage of the fillers can be statistically established by the use of multiple regressions and analysis of variances (ANOVA).

3. Results and discussion

3.1 Morphology of fillers and dispersion of fillers in the epoxy matrix

Apart from the thermal conductivity of the fillers, their shape, size, and distribution in the polymer matrix also affect the effective thermal conductivity of the obtained composite. The morphology of the as-received fillers is shown in the SEM images (Fig. 1). Talc nanoclay are platelet particles with a diameter median of 2 μm. A talc particle might be an aggregation of several layers, bonding to each other by weak van der Waals forces. ZnO particles are in hexagonal prism shape with sizes varying in the range of hundreds of nanometers.

The morphology of spherical BN cluster particles can be seen in Fig. 1(c) with an average diameter of 60 μm. The BN cluster particle consists of multiple platelet-like hexagonal BN

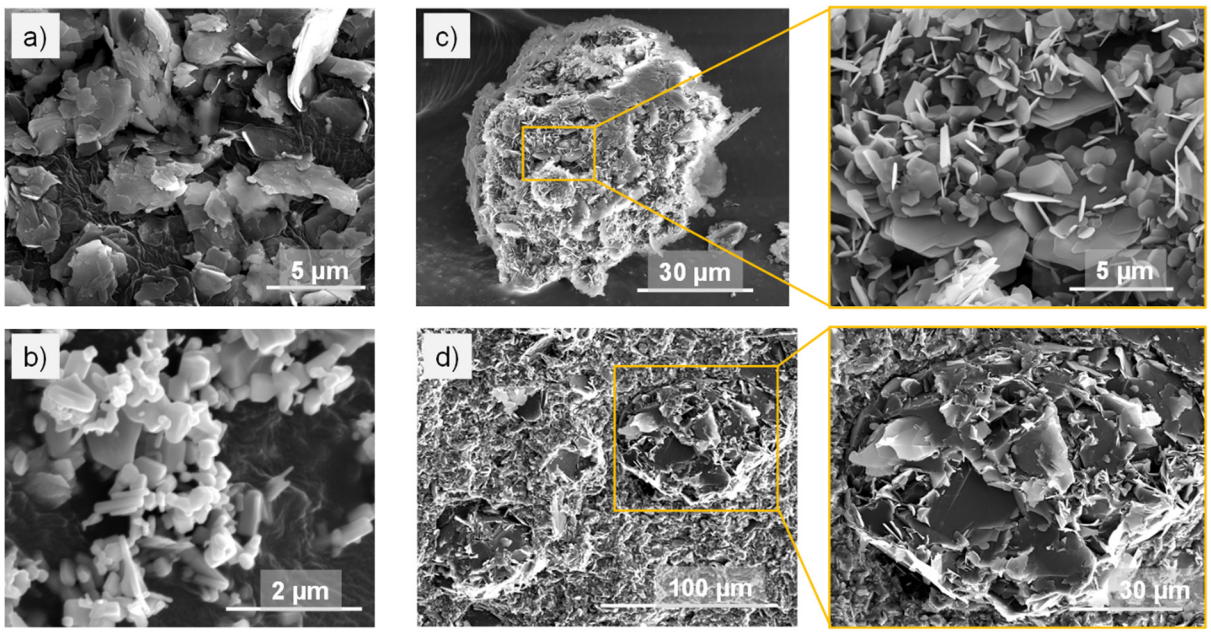

Fig. 1 SEM images of as-received functional fillers and an epoxy composite. (a) Talc platelets; (b) ZnO particles; (c) BN cluster particle PTX 60 with magnification showing edge-connecting BN platelets; (d) cross-section of an epoxy composite formulation, magnification – a BN cluster in the composite.

crystals which are held together at the edges in random orientations.

The distribution of the fillers in the epoxy matrix of a representative nanocomposite composed of X_1 = 60 wt%, X_2 = 20 wt%, X_3 = 12.5 wt%, and X_4 = 7.5 wt% is shown in an SEM image of a cross-section fracture (Fig. 1(d)). The EDX elemental mapping (Fig. 2) shows the distribution of C (which represents epoxy), Si (talc nanoclay), B and N (BN), and Zn (ZnO). It can be observed that the BN cluster particles preserve their original structure in the final composites, unlike how they were reported to be broken down into platelets during the processing elsewhere.[35] Talc and ZnO are observed to be homogeneously distributed between the BN particles. Overall, the functional fillers are well dispersed in the epoxy matrix. Thus, the heat flow in the composite can be ensured to be uniform.[36,37]

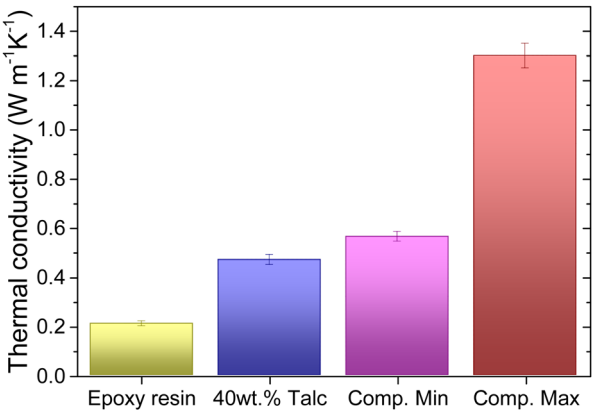

Fig. 3 Enhancement in thermal conductivity of the epoxy composite.

3.2 Design of experiments

3.2.1 Overview of thermal conductivity enhancement in the design space. An overview of the thermal conductivity results of the DoE design space is shown in Fig. 3. For comparison, neat epoxy resin and talc/epoxy composite with 40 wt% of talc (which is close to the processability limit) samples were fabricated. While the thermal conductivity of neat epoxy resin is only 0.2 W m^{-1} K^{-1} and that of the 40 wt% talc/epoxy composite is 0.48 W m^{-1} K^{-1}, the minimum thermal conductivity in the design space is 0.56 W m^{-1} K^{-1} corresponding to a formulation containing X_1 = 75 wt%, X_2 = 20 wt% and X_3 = 5 wt% (noted as Comp. Min). The maximum thermal conductivity is 1.3 W m^{-1} K^{-1}, which consists of X_1 = 60 wt%, X_2 = 20 wt%, and X_3 = 20 wt% BN (noted as Comp. Max). This maximum value is 6 times and 3 times higher than that of neat epoxy and the 40 wt% talc/epoxy composite, respectively.

3.2.2 Modelling the composite thermal conductivity based on the constituent contents. A quadratic (second-order) fitting model of the composite thermal conductivity was established through a regression process. The backward elimination fitting method has been conducted to select the predictor terms in the model. In this method, linear terms which represent additive effects of epoxy resin, talc nanoclay, BN cluster particles, and ZnO are forced in the model. The quadratic terms which express the nonlinear synergistic/antagonistic binary interaction effects of two components are chosen based on their statistical significance.

Various statistical data were used to analyze the mixture design. The *p*-value is an essential parameter to assess the null hypothesis, which states that there is no association between the term in the model and the output response. A good value of

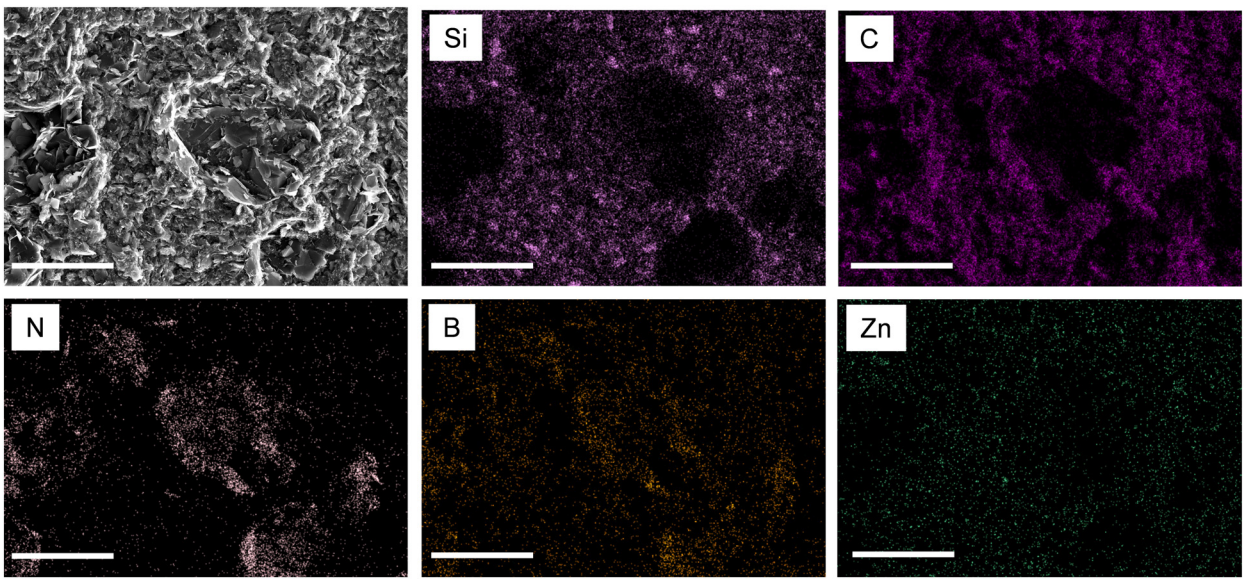

Fig. 2 SEM/EDX elemental mapping of a cross section fracture of the epoxy composite showing distribution of functional fillers in the epoxy matrix including SEM image of the selected area, C (represents epoxy), Si (represents talc nanoclay), B and N (represent BN), and Zn (represents ZnO). Scale bar: 50 μm.

Table 2 Estimated regression coefficients for the composite thermal conductivity

Term	Coef[a]	SE Coef[b]	T-Value[c]	p-Value
X_1	0.353	0.159	*	*
X_2	0.866	0.359	*	*
X_3	16.16	3.34	*	*
X_4	0.073	0.268	*	*
$X_1 \cdot X_3$	−14.93	5.41	−2.76	0.014
$X_2 \cdot X_3$	−13.91	4.90	−2.84	0.012

[a] Coefficient. [b] Standard error of the coefficient. [c] T-test.

significance level (α) to compare the p-value to is 0.05, which indicates that there is only a risk of 5% that there is an association between the term and the response. If the p-value ≤ 0.05, the term can be considered statistically significant. Otherwise, the term might not be significant and can be eliminated from the model.

In the backward elimination method, all the predictor terms (including linear and quadratic terms) are included at the beginning of the regression process. In each step, the least statistically significant term with a p-value ≥ 0.1 will be removed. The regression repeats until all remaining terms in the model have a p-value ≤ 0.05. After multiple regression steps, the model of the thermal conductivity of the epoxy composite depending on the percentile of the components in the experimental constraints has been established as shown in eqn (6). The coefficients of the quadratic model of the composite thermal conductivity, their standard error, and p-value are given in Table 2.

$$\lambda = 0.003527X_1 + 0.008663X_2 + 0.161606X_3 + 0.000726X_4 - 0.001493X_1 \cdot X_3 - 0.001391X_2 \cdot X_3 \quad (6)$$

The predicted response, shown in eqn (6) matches well with the experimental data with an R-squared of 98.17%. As a rule of thumb, the closer the R-squared to 100%, the better the model fits the experimental data. This high value of R-squared indicates the adequacy of the developed model. The ANOVA results are summarized in Table 3. The p-value for the regression of the composite thermal conductivity model is $p = 0.000$, in which the p-value of linear terms is 0.000 and the p-value of quadratic terms is 0.006, which is much less than 0.05. This states that all terms in the regression model have significant associations with the output response. Among the interaction terms in the model shown in eqn (6), only $X_1 \cdot X_3$ (epoxy and BN cluster particles) and $X_2 \cdot X_3$ (talc and BN cluster particles) show statistical significance with p-values of 0.014 and 0.012, respectively. All other interaction terms show statistical insignificance and thus are eliminated throughout the regression steps. Nevertheless, both $X_1 \cdot X_3$ and $X_2 \cdot X_3$ interaction terms have negative coefficients, demonstrating antagonistic effects between the two components.

Table 3 ANOVA for the composite thermal conductivity

Source	DF[a]	Seq SS[b]	Adj SS[c]	Adj MS[d]	F-Value[e]	p-Value
Regression	5	0.636132	0.636132	0.127226	171.68	0.000
Linear	3	0.625355	0.042060	0.014020	18.92	0.000
Quadratic	2	0.010777	0.010777	0.005389	7.27	0.006
$X_1 \cdot X_3$	1	0.004815	0.005646	0.005646	7.62	0.014
$X_2 \cdot X_3$	1	0.005963	0.005963	0.005963	8.05	0.012
Residual error	16	0.011857	0.011857	0.000741		
Total	21	0.647989				

[a] Degree of freedom. [b] Sequential sum of squares. [c] Adjusted sum of squares. [d] Adjusted mean of squares. [e] F test.

3.2.3 Experimental model validation. To verify the fitting model in eqn (6), a composite with the formulation consisting of X_1 = 60 wt%, X_2 = 26 wt%, X_3 = 11 wt%, and X_4 = 3 wt% was fabricated. The predicted value calculated using eqn (5) is 0.833 W m^{-1} K^{-1}, which shows a very small error of only 1.2% compared to the experimental value of 0.843 W m^{-1} K^{-1}.

3.2.4 Response contour and trace plots of composite thermal conductivity. Based on the mixture model shown in eqn (6), contour and trace plots of composite thermal conductivity were generated, as seen in Fig. 4 and 5, which provide insights into the relationship between the predicted composite thermal conductivity and the content of the mixture components. Fig. 4 shows the contour plots of the thermal conductivity, in which the points with the same predicted thermal conductivity are connected to form a contour line. Three cases are depicted with the total weight percentage of the organic fillers being 30 wt% (Fig. 4(a)), 35 wt% (Fig. 4(b)), and 40 wt% (Fig. 4(c)).

Fig. 5 displays the effects of all components in a single Cox response trace plot, showing how the output response changes compared to the reference blending when a mixture component content moves through the centroid point of the design space to the vertices while the remaining components are held in a constant ratio.[38] In the design space, the reference blend consists of X_1 = 63.3 wt%, X_2 = 25 wt%, X_3 = 8.3 wt% of BN, and X_4 = 3.33 wt%, with the composite thermal conductivity of 0.715 W m^{-1} K^{-1}.

3.2.5 Effects of individual inorganic fillers. As presented in eqn (6), BN cluster particles have the most influential impact on the composite thermal conductivity, showing a coefficient of 2–3 orders of magnitude higher than other components. The prevailing effects of BN cluster particles are also revealed on the contour plots (Fig. 4), where the thermal conductivity contours are parallel to solely the concentration of BN clusters. Moreover, as seen in Fig. 5, the response trace of the BN cluster in the studied range has the steepest slope, leading to an exponential increase in the composite thermal conductivity. This implies that by increasing the content of BN in the range up to 20 wt%, the filler-to-filler connection between the BN particles contributes to the enhancement of the composite thermal conductivity.

The coefficients of talc and ZnO in the model, shown in eqn (6) are relatively small. Also, as seen in Fig. 5, compared to the reference blend, ZnO and talc nanoclay has almost linear response traces with a relatively flat slope, indicating that an increase in the amount of these fillers has little influence on the composite thermal conductivity enhancement. Even though ZnO is reported to have a much higher thermal conductivity of 50 W m^{-1} K^{-1} [39] compared to talc (through-plane thermal

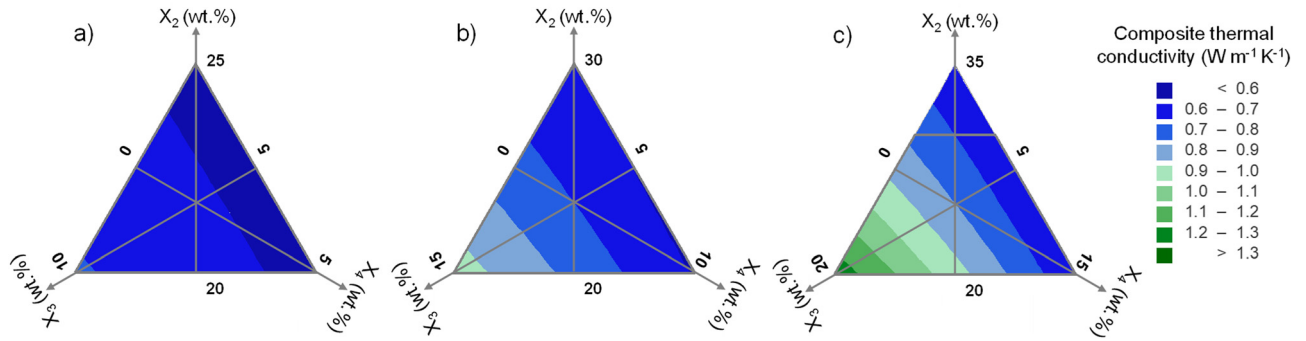

Fig. 4 Contour plots of composite thermal conductivity in three cases with the total content of fillers: (a) 30 wt%; (b) 35 wt%; (c) 40 wt%.

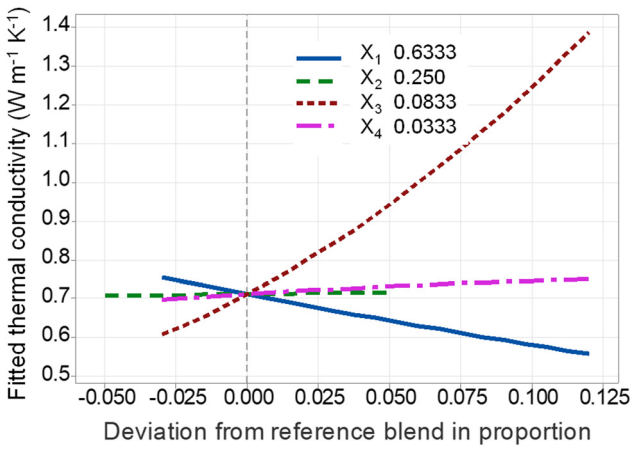

Fig. 5 Cox response trace plot showing the change of composite thermal conductivity referenced to centroid point of design space.

conductivity of talc is 1.76 W m^{-1} K^{-1} [40]), the slope of ZnO response trace is higher than that of talc nanoclay by only an incremental amount. This can be explained by the high density of ZnO, seen in Table 1, so that ZnO particles take only a small volume fraction. Moreover, the small size of ZnO particles is associated with high interfacial thermal resistance between the fillers and polymer matrix, which in turn hinders the thermal enhancement effects of ZnO particles.[38,41] On the other hand, compared to ZnO particles, talc with a 2D platelet structure provides a large contact area and the possibility of forming face-contact of the 2D platelet network, which promotes the composite thermal conductivity.[18,42]

3.2.6 Nonlinear binary interaction effects between the components. In the two interaction terms with statistical significance shown in eqn (6), the percentile of BN clusters appears in both terms due to the huge impact of this filler on the composite thermal conductivity. The antagonistic effects between BN cluster particles and 2D talc is unexpected, which counteract the possible synergistic effects between spherical and 2D particles.[43] Indeed, the experimental data show that when the content of talc increases by 5% from 20 wt% to 25 wt%, and to 30 wt% while the concentration of BN clusters is kept at 5 wt%, the composite thermal conductivity mildly increases from 0.564 W m^{-1} K^{-1} to 0.582 W m^{-1} K^{-1} (by 3.2%), and to 0.608 W m^{-1} K^{-1} (by 4.5%), respectively. A possible explanation is that the studied range of filler content is not of the range in which the synergistic effects would take place. Indeed, the hybrid composites show synergistic effects only in a strict range and content ratio between the fillers[35,44] when the secondary fillers, with different sizes and shapes, bridge the gaps that the primary filler cannot fill in to elongate the effective thermal conductive path. As seen in the SEM image in Fig. 2, the gap between adjacent BN clusters, which is filled with epoxy resin, talc, and ZnO, is still large. Therefore, the antagonistic effects between BN clusters and talc, as well as between BN clusters and epoxy resin, limit the enhancement of composite thermal conductivity.

3.2.7 Effects of total fillers concentration. The DoE analysis shows that the higher total content of fillers leads to the higher thermal conductivity of the composite. For example, with 30 wt%, 35 wt%, and 40 wt% of total fillers, the composite thermal conductivity could reach 0.7 W m^{-1} K^{-1}, 0.9 W m^{-1} K^{-1}, and 1.3 W m^{-1} K^{-1}, respectively, as seen in Fig. 4. The increase of the composite thermal conductivity along with the increase in the filler content follows theoretical predictions, for example proposed by Cheng-Vachon,[45] Lewis-Nielsen,[46] and Agari–Uno.[47,48] According to these theories, by increasing the content of fillers, and, also decreasing the volume of epoxy resin which acts as a thermal barrier, the effective length of the conductive paths created by the organic fillers in the composite is much elongated.

3.3 Effects of BN cluster particles on the composite thermal conductivity enhancement

In the spherical BN cluster particles, BN nanosheets are randomly orientated and edge-connected, which is believed to be the key to the enhanced thermal conductivity of the composite. To demonstrate and elucidate the critical role of structured heat conducting paths endowed in BN clusters, the composites with BN clusters are compared to that with homogeneously dispersed BN platelets. Theoretical prediction models of filled composites are implemented to estimate the effective thermal conductivity of BN clusters and BN platelets based on the obtained experimental data.

Various models have been proposed to predict the thermal conductivity of filled composites (λ). The essential parameters

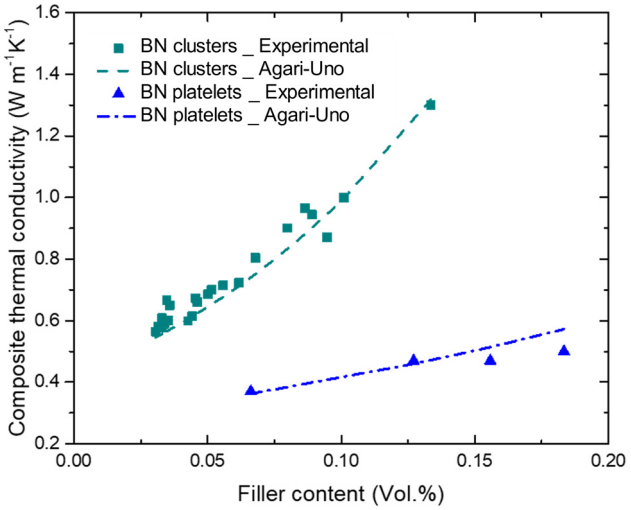

Fig. 6 Thermal conductivity of epoxy/BN clusters and epoxy/BN platelets composite and fits for the Agari–Uno model.

taken into the models are thermal conductivity of polymer matrix λ_m and fillers λ_f, and volume content of fillers φ. According to the Agari–Uno model,[47,48] the thermal conductivity of a composite can be calculated as shown in eqn (7).

$$\ln(\lambda) = \varphi C_2 \ln(\lambda_m) + (1 - \varphi)\ln(C_1\lambda_f) \quad (7)$$

where C_1 and C_2 are adjustable constants.

The experimental data and fitted curves applying the Agari–Uno model in both cases of epoxy/spherical BN clusters and epoxy/BN platelets composite are shown in Fig. 6. It can be seen that the thermal conductivity of epoxy/BN platelets is much lower than that of the BN cluster at the same filler content. For instance, at a filler content of 13 vol%, the thermal conductivity of epoxy/BN platelets is only $\sim$0.5 W m^{-1} K^{-1}, while that of the epoxy/BN cluster is 1.3 W m^{-1} K^{-1}. Applying C_1 = 1.4 and C_2 = 1.32, given in ref. 44 to eqn (7), good agreements between the experimental and fitted values are achieved with effective thermal conductivity of spherical BN clusters $\lambda_{f\_BN\ cluster}$ = 100 W m^{-1} K^{-1}, which is one order of magnitude higher than that of dispersed BN platelets being $\lambda_{f\_BN\ platelet}$ = 7 W m^{-1} K^{-1}.

As shown from the above analytical results, given the same volume content, the structure of the BN fillers has a significant effect on the composite thermal conductivity. The discrepancy in thermal conductive paths of the two structures of BN nanosheets is illustrated in Fig. 7. BN nanosheets are known to possess strongly anisotropic thermal conductivity (see Table 1). In a well-manufactured epoxy/BN platelets composite, most BN nanosheets are intercalated by epoxy resin. The heat transfer through the composite is accomplished *via* multiple successive modules: epoxy- interface-BN nanosheet-interface, demonstrated in Fig. 7(a). Because BN nanosheets are more likely to align with a preferred orientation parallel to the sample surface, the through-thickness thermal conductivity is relatively low. Moreover, the interface between epoxy matrix and BN nanosheets causes considerable interfacial thermal resistance. The estimated effective thermal conductivity of dispersed BN platelets is higher than the through-plane value due to, probably, local face-contact between BN nanosheets,[18,42] which creates a network with higher thermal conductivity.

On the other hand, in spherical BN clusters, the BN nanosheets are held together by the edges to form a network, depicted in Fig. 7(b). Therefore, effective thermal conduction paths are created throughout the cluster. Moreover, the size of BN clusters is much larger than the individual platelets. This reduces not only the interfacial thermal resistance, but also the number of interfaces between epoxy and filler, compared to the epoxy/BN platelets composite with the same filler volume content. Thanks to the random orientation of the BN nanosheets, the spherical BN clusters obtain more isotropic thermal conductivity, which means that the thermal conductive pathway will be independent of the particle orientation.

However, the estimated effective thermal conductivity of BN clusters is less than the in-plane thermal conductivity of BN. This might be due to contact thermal resistance between the BN nanosheets, as illustrated in Fig. 7(b), which reduces the effective thermal conductivity of the BN cluster.

3.4 Dielectric properties

Incorporating inorganic fillers into polymer matrices could lead to undesirably degraded dielectric properties,[49,50] which

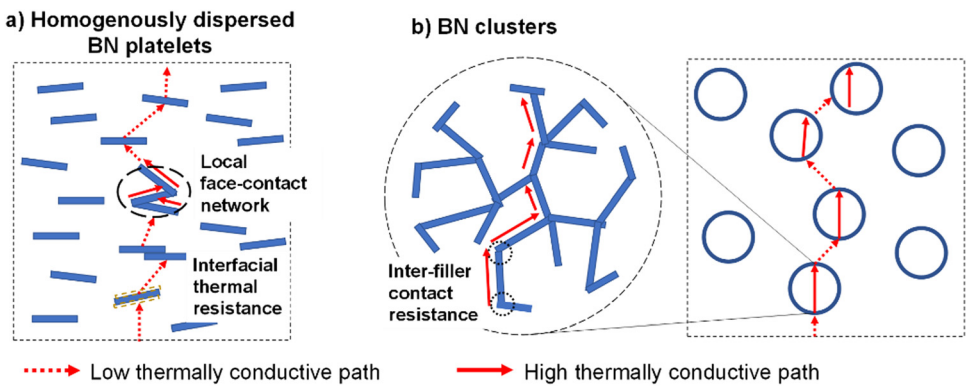

Fig. 7 Schematic diagrams of thermally conductive paths of the epoxy composite in two cases: (a) with homogeneously dispersed BN platelets; (b) with spherical BN cluster particles.

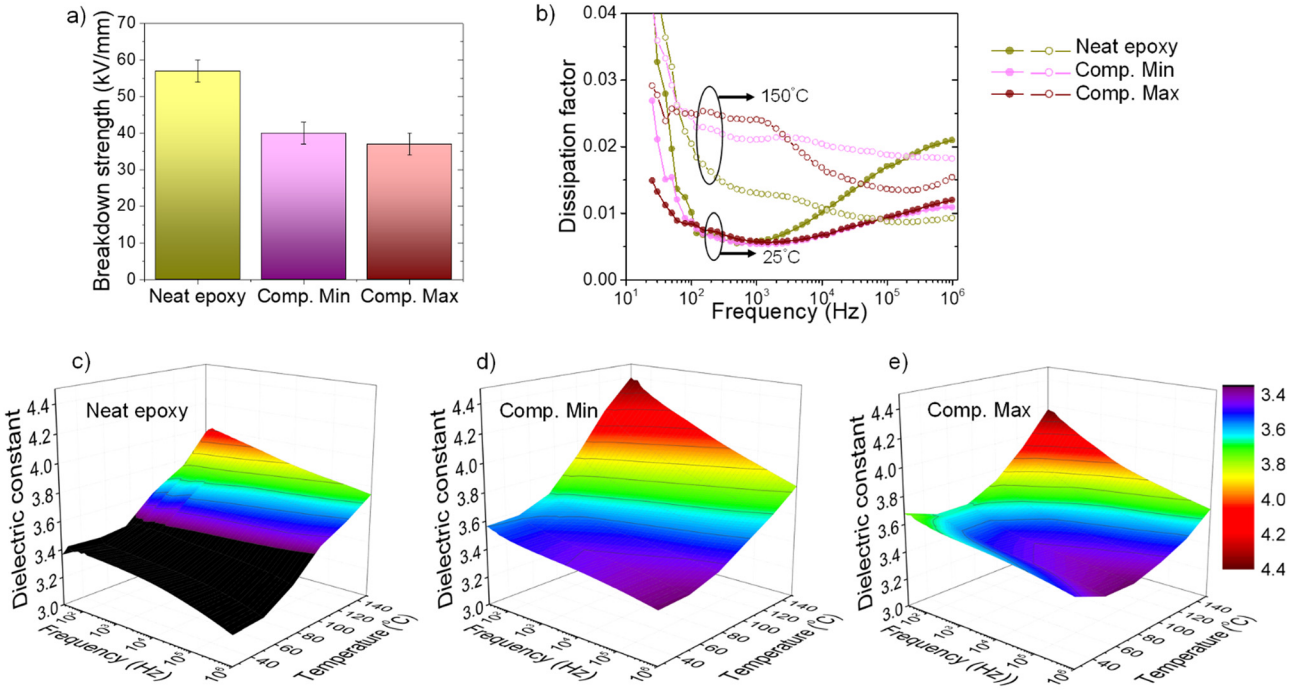

Fig. 8 Dielectric properties of developed composites benchmarking neat epoxy resin. (a) Dielectric breakdown strength; (b) dissipation factor at 25 °C and 150 °C; (c–e) dielectric constant of neat epoxy, Comp. Min, and Comp. Max, respectively.

are not suitable for electrical insulation, especially in high voltage applications. Potential lowering of the breakdown strength and upsurging dissipation factor (loss) could lead to excessive wasted heat generation and a rising dielectric constant which distorts electrical field distribution. We demonstrate that the dielectric properties of the developed thermally conductive composites are well qualified for high-performance electrical applications. Fig. 8 summarizes the dielectric properties of representatives – Comp. Min and Comp. Max, benchmarking the neat epoxy resin.

The dielectric breakdown strengths of Comp. Min and Comp. Max are maintained at 40 kV mm^{-1}, as seen in Fig. 8(a). This high breakdown strength is well suited for rotating machine industries and higher than that of the micaceous (mica, epoxy, glass–fabric composite) insulation. The dissipation factors at 25 °C of the composites are comparable to the neat epoxy resin as presented in Fig. 8(b). At 150 °C, the dissipation factors of the composites remain less than 3% in a wide frequency range of 30–10^6 Hz. The dielectric constants of the composites are slightly higher than the neat epoxy and are as low as 4.4 over the entire studied temperature and frequency ranges. Both the dielectric dissipation and dielectric constants of these composites are lower than the state-of-the-art micaceous insulation for rotating machines.[5,51]

4. Conclusion

In this paper, the effects of a hybrid filler system with different size, shape, and thermal conductivity on the effective thermal conductivity of the epoxy composite have been investigated using the statistical model of the Minitab software package. A thermal conductivity model of the epoxy composite with an *R*-squared of 98.17% has been established based on the concentration of epoxy resin, talc, BN cluster, and ZnO.

In the studied constraint, increasing the content of fillers leads to an increase in the thermal conductivity of the composites. However, depending on the filler properties, the effects that each filler contribute to the thermal conductivity enhancement of the epoxy composite are different. ZnO particles, with the content ranging from 0 to 15 wt%, possessing a high thermal conductivity of 50 W m^{-1} K^{-1}, yet with small sizes and high density, show limited effects on increasing the thermal conductivity of the composites. Similarly, the response trace of 2D talc nanoclay has a relatively flat slope in the composite thermal conductivity in the range of 20–30 wt%.

The spherical BN cluster particles, possessing the highest thermal conductivity and largest size, demonstrate the most effective thermal conductivity enhancement. In the range of 5–20 wt%, BN clusters could lead to an exponential increase in the effective thermal conductivity.

The prevailing enhancement in the composite thermal conductivity of spherical BN clusters is attributed to the effective thermal conductive path, created by structured edge-connecting nanosheets, in which heat is transferred in the high thermally conductive in-plane BN nanosheets. BN clusters showed one order of magnitude higher effective thermal conductivity compared to homogeneously dispersed BN platelets at the same filler contents.

The cooperation of hybrid fillers into an epoxy matrix results in 6× enhancement in thermal conductivity compared to the

neat epoxy resin. Additionally, the designed epoxy composites possess a high dielectric breakdown strength of >40 kV mm^{-1}, low dielectric constant, and low dissipation factor, which are favorable for a wide range of industrial applications.

Conflicts of interest

There are no conflicts to declare.

Acknowledgements

The authors acknowledge the kind support from the U.S. Office of Naval Research under Grant N00014-15-1-2413 and Grant N00014-19-1-2306.

Notes and references

1 B. Ellis, *Chemistry and Technology of Epoxy Resins*, Springer, Netherlands, Dordrecht, 1993.
2 S. Rimdusit and H. Ishida, *Polymer*, 2000, **41**, 7941–7949.
3 Y. He, B. E. Moreira, A. Overson, S. H. Nakamura, C. Bider and J. F. Briscoe, *Thermochim. Acta*, 2000, **357–358**, 1–8.
4 M. Uno, K. Ogawa, Y. Takeda, Y. Sone, K. Tanaka, M. Mita and H. Saito, *J. Power Sources*, 2011, **196**, 8755–8763.
5 H. H. Nguyen, A. Y. Mirza, W. Chen, Y. Liu, J. Ronzello, J. Chapman, A. M. Bazzi and Y. Cao, *IEEE Access*, 2021, **9**, 2274–2282.
6 H. Nguyen, Y. Liu, W. Chen, M. Ghassemi, J. Chapman, A. Bazzi and Y. Cao, *IEEE Electric Ship Technologies Symposium*, *ESTS*, 2017, pp. 274–279.
7 G. Stone, E. A. Boutler, I. Gilbert and H. Dhirani, *Electrical Insulation for Rotating Machines*, Wiley/IEEE press, 2004.
8 I. H. Tavman, *Powder Technol.*, 1997, **91**, 63–67.
9 N. M. Sofian, M. Rusu, R. Neagu and E. Neagu, *J. Thermoplast. Compos. Mater.*, 2001, **14**, 20–33.
10 W. Kowbel, C. Bruce, K. Tsou, K. Patel, J. Withers and G. Youngblood, *J. Nucl. Mater.*, 2000, **283–287**, 570–573.
11 S. Yoshihara, M. Tokita, T. Ezaki, M. Nakamura, M. Sakaguchi, K. Matsumoto and J. Watanabe, *J. Appl. Polym. Sci.*, 2014, **131**(6), DOI: 10.1002/app.39896.
12 B. Maira, K. Takeuchi, P. Chammingkwan, M. Terano and T. Taniike, *Compos. Sci. Technol.*, 2018, **165**, 259–265.
13 B. Lee and G. Dai, *J. Mater. Sci.*, 2009, **44**, 4848–4855.
14 C. P. Wong and R. S. Bollampally, *J. Appl. Polym. Sci.*, 1999, **74**, 3396–3403.
15 M. E. Meibodi, M. Vafaie-Sefti, A. M. Rashidi, A. Amrollahi, M. Tabasi and H. S. Kalal, *Int. Commun. Heat Mass Transf.*, 2010, **37**, 319–323.
16 J. Nanda, C. Maranville, S. C. Bollin, D. Sawall, H. Ohtani, J. T. Remillard and J. M. Ginder, *J. Phys. Chem. C*, 2008, **112**, 654–658.
17 S. Ganguli, A. K. Roy and D. P. Anderson, *Carbon N. Y.*, 2008, **46**, 806–817.
18 C. Huang, X. Qian and R. Yang, *Mater. Sci. Eng., R*, 2018, **132**, 1–22.
19 B. L. Zhu, J. Wang, H. Zheng, J. Ma, J. Wu, Z. H. Gan and J. Liu, *J. Alloys Compd.*, 2017, **701**, 499–507.
20 B. L. Zhu, J. Wang, H. Zheng, J. Ma, J. Wu and R. Wu, *Composites, Part B*, 2015, **69**, 496–506.
21 Y. Cao, P. C. Irwin and K. Younsi, *IEEE Trans. Dielectr. Electr. Insul.*, 2004, **11**, 797–807.
22 P. Jiang, X. Qian, R. Yang and L. Lindsay, *Phys. Rev. Mater.*, 2018, **2**, 1–8.
23 Q. Cai, D. Scullion, W. Gan, A. Falin, S. Zhang, K. Watanabe, T. Taniguchi, Y. Chen, E. J. G. Santos and L. H. Li, *Sci. Adv.*, 2019, **5**, 1–9.
24 S. N. Paisner, P. J. Hans and P. Meneghetti, *US Pat.*, US7524560B2, 2009.
25 A. Gowda, S. N. Paisner, S. Tonapi, P. Meneghetti, P. Hans, G. Strosaker, A. Acharya, K. Nagarkar and K. Srihari, Proc. 7th Electron. Packag. Technol. Conf. EPTC 2005, 2005, 2, 683–690.
26 H. Chen, V. V. Ginzburg, J. Yang, Y. Yang, W. Liu, Y. Huang, L. Du and B. Chen, *Prog. Polym. Sci.*, 2016, **59**, 41–85.
27 M. J. Anderson and P. J. Whitcomb, *Rubber Plast. News*, 2002, 16–17.
28 R. P. Niedz and T. J. Evens, *In Vitro Cell. Dev. Biol.: Plant*, 2011, **47**, 682–694.
29 L. Ayed, S. Achour and A. Bakhrouf, *Water SA*, 2011, **37**, 21–26.
30 S. Damiri, H. R. Pouretedal and O. Bakhshi, *Chem. Eng. Res. Des.*, 2016, **112**, 155–162.
31 Z. Jeirani, B. Mohamed Jan, B. Si Ali, I. Mohd. Noor, S. Chun Hwa and W. Saphanuchart, *Chemom. Intell. Lab. Syst.*, 2012, **112**, 1–7.
32 P. M. Murray, F. Bellany, L. Benhamou, D.-K. Bučar, A. B. Tabor and T. D. Sheppard, *Org. Biomol. Chem.*, 2016, **14**, 2373–2384.
33 TA Instruments-DTC 300-Thermal conductivity meter - Getting started guide, 2013.
34 R. A. McLean and V. L. Anderson, *Technometrics*, 1966, **8**, 447–454.
35 S. N. Leung, M. O. Khan, E. Chan, H. E. Naguib, F. Dawson, V. Adinkrah and L. Lakatos-Hayward, *J. Appl. Polym. Sci.*, 2013, **127**, 3293–3301.
36 Y. S. Song and J. R. Youn, *Carbon N. Y.*, 2005, **43**, 1378–1385.
37 A. Tessema, D. Zhao, J. Moll, S. Xu, R. Yang, C. Li, S. K. Kumar and A. Kidane, *Polym. Test.*, 2017, **57**, 101–106.
38 D. R. Cox, *Biometrika*, 1971, **58**, 155–159.
39 X. Wu, J. Lee, V. Varshney, J. L. Wohlwend, A. K. Roy and T. Luo, *Sci. Rep.*, 2016, **6**, 1–10.
40 C. Clauser and E. Huenges, *Thermal Conductivity of Rocks and Minerals*, in *Rock Physics & Phase Relations: A Handbook of Physical Constants*, ed. T. J. Ahrens, American Geophysical Union, Washington DC, 2013, pp. 105–126, DOI: http://dx.doi.org/10.1029/RF003p0105.
41 S. Yu, S. Yang and M. Cho, *J. Appl. Phys.*, 2013, **114**, 213503.
42 J. Tielke, M. Maas, M. Castillo, K. Rezwan and M. Avila, *Proc. R. Soc. A Math. Phys. Eng. Sci.*, 2021, **477**(2250), DOI: 10.1098/rspa.2021.0222.

43 Z. Li, D. Ju, L. Han and L. Dong, *Thermochim. Acta*, 2017, **652**, 9–16.
44 K. Gaska, A. Rybak, C. Kapusta, R. Sekula and A. Siwek, *Polym. Adv. Technol.*, 2015, **26**, 26–31.
45 C. P. Wong and R. S. Bollampally, *IEEE Trans. Adv. Packag.*, 1999, **22**, 54–59.
46 L. E. Nielsen, *Ind. Eng. Chem. Fundam.*, 1974, **13**, 17–20.
47 Y. Agari and T. Uno, *J. Appl. Polym. Sci.*, 1986, **32** 5705–5712.
48 Y. Agari, A. Ueda and S. Nagai, *J. Appl. Polym. Sci.*, 1991, **42**, 1665–1669.
49 Z. Cai, X. Wang, B. Luo, W. Hong, L. Wu and L. Li, *Compos. Sci. Technol.*, 2017, **145**, 105–113.
50 R. Wang, C. Xie, S. Luo, B. Gou, H. Xu and L. Zeng, *RSC Adv.*, 2019, **9**, 19648–19656.
51 H. Nguyen, Y. Wang, J. Ronzello, J. Chapman and Y. Cao, *2019 IEEE Electric Ship Technologies Symposium (ESTS)*, IEEE, 2019, pp. 189–194.